ErbB2 is required for ductal morphogenesis of the mammary gland

Amy J. Jackson-Fisher*, Gary Bellinger*, Rajani Ramabhadran*, Jacqueline K. Morris†, Kuo-Fen Lee‡, and David F. Stern*§

*Department of Pathology, Yale University School of Medicine, New Haven, CT 06520-8023; †Department of Biology and Geology, Baldwin-Wallace College, Berea, OH 44017; and ‡The Salk Institute, 10010 North Torrey Pines Road, La Jolla, CA 92037

Edited by Joan S. Brugge, Harvard Medical School, Boston, MA, and approved October 25, 2004 (received for review September 24, 2004)

The *ERBB2/HER2/NEU* receptor tyrosine kinase gene is amplified in up to 30% of human breast cancers. The frequent and specific selection of this receptor kinase gene for amplification in breast cancer implies that it has important normal functions in the mammary gland. To investigate the functions of ErbB2 during normal mouse mammary gland development, we transplanted mammary buds from genetically rescued *ErbB2*$^{-/-}$ embryos that express ErbB2 in the cardiac muscle. *ErbB2*$^{-/-}$ mammary buds transplanted to a wild-type mammary fat pad support outgrowth of an epithelial tree that advances only slowly through the mammary fat pad at puberty. This penetration defect is associated with structural defects in terminal end buds, characterized by a decrease in body cell number, an increased presence of cap-like cells in the prelumenal compartment, and the presence of large luminal spaces. Lobuloalveolar development was not affected in glands that developed from *ErbB2*$^{-/-}$ transplanted tissue. The results may have implications for the aggressive phenotypes associated with *ERBB2*-overexpressing mammary carcinomas.

development | terminal end bud | HER2 | EGF

The protooncogene *ERBB2/HER2/NEU* encodes a receptor tyrosine kinase of the epidermal growth factor receptor (EGFR) family, which includes *EGFR/ERBB1/HER1*, *ERBB2/HER2/NEunits*, *ERBB3/HER3*, and *ERBB4/HER4*. *ERBB2* is amplified in up to 30% of human breast cancers (1). Amplification and overexpression of *ERBB2* are associated with poorer prognosis of breast cancer patients (1–3). ERBB2 is the target for the therapeutic antibody Herceptin (trastuzumab), which is used for treatment of women with advanced breast cancer that overexpresses ERBB2 (4). The preferential amplification of *ERBB2* in breast cancer, relative to other receptor tyrosine kinase genes, and the association with poor prognosis imply that activated ErbB2 has powerful and pleiotropic carcinogenic properties. Indeed, in contrast to some oncogenes, *ERBB2* promotes invasion and metastasis, in addition to excessive proliferation (5, 6). Moreover, in mouse models, activated *ERBB2* is especially potent in induction of metastatic mammary carcinoma (7, 8). The preferential association of ERBB2 amplification with mammary and ovarian carcinomas suggests that these properties reflect important normal functions for *ERBB2* in these endocrine-responsive tissues.

ErbB2 is an orphan receptor that is unable to bind conventional growth factors on its own (reviewed in ref. 9). However, ErbB2 forms heteromers with ligand-activated EGFR, ErbB3, and ErbB4, which enables ErbB2 to respond to the ≈13 EGF- and neuregulin-like growth factors. The ErbBs are promiscuous in their ability to form heteromeric complexes, but ErbB2 is a preferred dimerization partner that is generally coexpressed with other ErbBs (10–13). In this capacity, it may function as a common ErbB subunit that augments signaling power and diversity, through its ability to couple to specific substrates and to alter down-regulation pathways of other ErbBs.

Despite the link of *ERBB2* to tumorigenesis, the roles of *ERBB2* in normal mammary gland development are unknown. The overlapping expression pattern of the four ErbBs and multiple ErbB ligands has made it difficult to interpret the physiological function of any individual ErbB (reviewed in ref. 14). In pubescent female mice at 5 weeks of age, both ErbB2 and EGFR proteins are expressed in the major cell compartments of the mammary gland. By 8 weeks of age, ErbB2 is especially prominent in the epithelium and reduced in the stroma, whereas EGFR is localized to the stroma (15). Both EGFR and ErbB2 are Tyr-phosphorylated at puberty in the mouse mammary gland, indicating that they are functionally activated (16). ErbB3 and ErbB4 are expressed at low levels before maturity but are expressed at higher levels during pregnancy and lactation (15, 16). ErbB2 expression has been detected at later stages of development as well. All four ErbBs were detected in mammary glands of mice in late pregnancy and early lactation. EGFR and ErbB2 proteins are expressed in the lobuloalveolar epithelium, whereas ErbB3 and ErbB4 are enriched in the ducts (15).

The timing of expression and Tyr phosphorylation of ErbB2 during mammary development suggests roles for ErbB2 in the nulliparous gland at puberty, during late pregnancy, and during early lactation. The phenotype of transgenic mice expressing a truncated dominant-negative *ErbB2* in adult females, which retards late mammary development and lactation, has suggested an important role for ErbB2 in final stages of lactational differentiation (17). However, the ability of ErbB2 to form heteromers with other EGF family receptors means that the dominant-negative effects may be mediated through inactivation of endogenous ErbB2, other ErbBs, or some combination.

Determination of the *ErbB2*$^{-/-}$ mammary phenotype has been hampered by early embryonic lethality due to a cardiac defect (18, 19). This defect can be genetically rescued by tissue-specific expression of a rat *neu/ErbB2* transgene targeted to cardiac muscle, yet the *ErbB2*$^{-/-}$ mice still die at birth because of loss of innervation of the diaphragm (20, 21). We have determined the consequences of inactivating murine *ErbB2* by transplanting embryonic mammary buds from the genetically rescued *ErbB2*$^{-/-}$ transgenic mice into the cleared mammary fat pads of immature female mice. Transplanted *ErbB2*$^{-/-}$ mammary buds support outgrowth of an epithelial tree in a wild-type mammary fat pad. However, there are substantial delays in ductal penetration. The growth defect is associated with structural defects in terminal end buds (TEBs), characterized by a decrease in body cell number, an increased presence of cap-like cells in the prelumenal compartment, and the presence of large luminal spaces.

Materials and Methods

Mammary Gland Transplants. Embryonic day (E) 12.5–E15.5 embryos (stage estimated from vaginal plugging, timed pregnancies,

This paper was submitted directly (Track II) to the PNAS office.

Abbreviations: TEB, terminal end bud; EGFR, epidermal growth factor receptor; IHC, immunohistochemistry; SMA, smooth muscle actin; MMP, matrix-metalloproteinase.

§To whom correspondence should be addressed. E-mail: df.stern@yale.edu.

© 2004 by The National Academy of Sciences of the USA

and/or appearance of embryos) resulting from intercross of compound heterozygotes for an α-myosin heavy chain (α-MHC) promoter rat *neu*/*ErbB2* cDNA transgene and $ErbB^{+/-}$ in a mixed 129/BALB/c/ICR strain background (20) were harvested by Caesarean section. The embryos were maintained in DMEM/10% FCS overnight while sex (*SRY* gene in males) and *ErbB2* genotypes were determined by PCR. Three-week-old immunocompromised $Rag1^{-/-}$ mice were cleared of endogenous epithelium in the no. 4 inguinal mammary fat pads by removing the tissue between the nipple and the lymph node (22). The excised portions of recipient glands were whole-mounted and stained with carmine alum to verify clearing of the epithelium. For each recipient mouse, one no. 4 inguinal mammary fat pad was transplanted with a single mammary bud isolated from a cardiac-rescued MHC-*ErbB2* $ErbB2^{-/-}$ female, and the contralateral no. 4 inguinal fat pad was transplanted with a mammary bud from an $ErbB2^{+/+}$ or $ErbB2^{+/-}$ female littermate. The fat pads containing transplants were harvested from virgin hosts at 4, 7, or 13 weeks posttransplantation, or the recipients were bred and the glands harvested at 1 day postpartum or after various points after gland remodeling. The overall take rate for transplanted buds was 46% and was not affected by the genotype of the donor embryo. All animal work was approved by the Yale University Institutional Animal Care and Use Committee.

Morphological Analysis. For whole-mount analysis, mammary glands were fixed in acetic acid/ethanol and cleared with acetone, and the ductal tree was visualized by staining with carmine alum as described (23). The number of whole mounts analyzed was six +/+ or +/− and six −/− late pregnancy fetuses or newborn pups, six +/+ and two −/− gland outgrowths at 4 weeks after transplantation, four +/+ and six −/− glands 7 weeks after transplantation, four +/+ and four −/− glands at 13 weeks after transplantation, seven +/+ or +/− and six −/− glands at 1 day postpartum (uniparous and multiparous), and two +/+ or +/− and two −/− parous nonpregnant adults.

For histological analysis, mammary glands were placed in freshly prepared 4% paraformaldehyde for 3 h to overnight at 4°C, subjected to a series of ethanol washes with up to 70% ethanol, and embedded in paraffin. Five-micrometer sections were cut and stained with hematoxylin/eosin (H&E) (17). Twelve +/+, four +/−, and seven −/− gland outgrowths were analyzed 4 weeks posttransplant; six +/+ or +/− and nine −/− glands at 7 weeks posttransplant; one +/+ and two −/− glands at 13 weeks posttransplant; and five +/+ or +/− and four −/− glands at 1 day postpartum (uniparous and multiparous).

To determine total ductal outgrowth length, digital images of each whole gland or half gland stained with carmine alum were imported into NIH imaging software. A line was drawn along the longest axis of ductal growth and measured in arbitrary units. The measurements for all of the glands were averaged, and the standard deviation was determined. To determine the branch density, digital images of the whole gland or half gland stained with carmine alum were analyzed by using NIH IMAGEJ. The number of branch points was determined within a box of fixed dimensions. The statistical significance was determined by Student's *t* test.

Immunohistochemistry. Mouse monoclonal anti-E-cadherin clone 36 (Transduction Laboratories, Lexington, KY), mouse monoclonal anti-α Smooth Muscle Actin clone 1A4 (Sigma Immuno Chemicals), goat polyclonal P-cadherin (N-19) (Santa Cruz Biotechnology), and rabbit polyclonal neogenin (H-175) (Santa Cruz Biotechnology) were used. For E-cadherin immunohistochemistry (IHC) (n = 4 +/+ and 6 −/− glands), the mouse-on-mouse staining procedure (Vector Laboratories) was followed, with microwave antigen unmasking in antigen unmasking solution (Vector Laboratories) and a 1:300 dilution of primary antibody. For smooth muscle actin (SMA) IHC (n = 6 +/+ and 6 −/− glands), the mouse-on-mouse staining procedure was followed, with a 1:1,000 dilution of primary antibody. Mouse IgG was used as a negative control for both E-cadherin and SMA IHC. For P-cadherin IHC (n = 6 +/+ and 4 −/− glands), the TSA Biotin System kits protocol for IHC (PerkinElmer) was used, with a 1:400 dilution of primary antibody. Goat IgG was used as a negative control for P-cadherin IHC. For neogenin IHC (n = 5 +/+ and 5 −/− glands), the DAKO catalyzed signal amplification (CSA) system, peroxidase, and the DAKO CSA ancillary system were used (DAKO), with the provided anti-mouse link replaced with the CSA Rabbit Link (DAKO) and with a 1:1,000 dilution of primary antibody. Mammary gland tissue from $neogenin^{-/-}$ mice was only very minimally stained with anti-neogenin. Rabbit IgG was also used as a negative control for neogenin IHC.

Fig. 1. Whole-mount analysis of prenatal mammary gland development. Shown are no. 4 inguinal mammary glands from female embryos harvested late in pregnancy. (*a*) $ErbB2^{+/-}$ embryos have a typical rudimentary ductal tree attached to the nipple (left) with few branches. (*b*) The $ErbB2^{-/-}$ littermate embryo has a ductal tree emanating from the nipple, with an increased number of branches.

BrdUrd and TUNEL. For BrdUrd analysis (n = 8 +/+ and 4 −/− glands), mice were injected with cell proliferation labeling reagent (Amersham Pharmacia) 2 h before killing. A 1:10 dilution of anti-BrdUrd-POD (monoclonal antibody to the thymidine analogue 5-bromo-2′-deoxyuridine, Fab fragments with peroxidase conjugated) (Roche) was used as described (24). For TUNEL analysis, the *in situ* cell death detection kit (Fluorescein) (Roche) was used according to the manufacturer's instructions.

Results

$ErbB2^{-/-}$ mice die mid-gestation (around day 10.5) because of a failure of ventricular trabeculation (18, 19). The cardiac defect can be bypassed by using a transgene with a cardiac-specific α-myosin heavy chain promoter expression driving expression of a rat *ErbB2* cDNA in the myocardium (20, 21). These "cardiac-rescued" $ErbB2^{-/-}$ mice die at birth from respiratory arrest. In late-stage embryos and perinatally, cardiac-rescued $ErbB2^{-/-}$ mammary glands are grossly normal (Fig. 1*b*). Hence, *ErbB2* is not absolutely required in the epithelium or stroma for prenatal mammary gland development.

The contribution of *ErbB2* to postnatal mammary development was evaluated by transplanting mammary buds from cardiac-rescued $ErbB2^{-/-}$ mice [embryonic day (E) 13.5–E15.5] into cleared mammary fat pads of prepubescent 3-week-old immunocompromised $Rag1^{-/-}$ mice. The contralateral fat pad received buds from homozygous (+/+) or heterozygous littermates. In virgin animals, ductal outgrowth of glands reconstituted with $ErbB2^{-/-}$ tissue was defective (Fig. 2). $ErbB2^{+/+}$ outgrowths typically filled the fat pad within 4 weeks of transplantation (Fig. 2 *a*, *c*, and *e*), whereas ductal penetration by $ErbB2^{-/-}$ tissue was incomplete, even after 7 weeks (Fig. 2 *b* and *d*). By 13 weeks, ductal penetration of

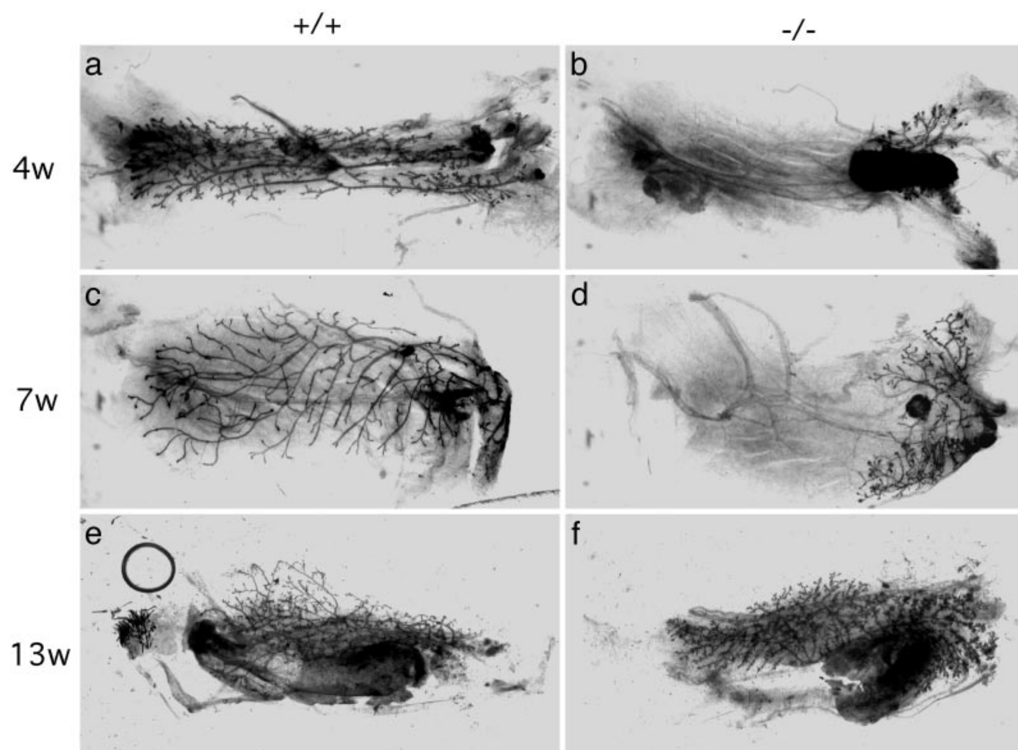

Fig. 2. Whole-mount analysis of ductal morphogenesis in transplanted glands from virgin female animals. Paired mammary buds from *ErbB2*$^{+/+}$ and *ErbB2*$^{-/-}$ day 13.5 embryos were transplanted into contralateral cleared mammary fat pads of 3-week-old *Rag1*$^{-/-}$ females. The glands were harvested 4 weeks (*a* and *b*), 7 weeks (*c* and *d*), or 13 weeks (*e* and *f*) posttransplantation. Pairs of glands shown at each time point are from littermate donors and the same recipient mouse.

ErbB2$^{-/-}$ mammary glands ranged from three-quarters full to completely filled (Fig. 2*f*). When compared pairwise in the same recipient females, outgrowths from *ErbB2*$^{+/+}$ donors were, on average, 67% longer than outgrowths from *ErbB2*$^{-/-}$ donors (Table 1 and Fig. 2). At 7 weeks posttransplantation, the number of branch points per unit area was higher in the *ErbB2*$^{-/-}$ transplants than the *ErbB2*$^{+/+}$ transplants, indicating an increase in branching in the *ErbB2*$^{-/-}$ transplants (Table 1). In the majority of the transplant recipients analyzed after pregnancy, the *ErbB2*$^{-/-}$ and *ErbB2*$^{+/+}$ glands filled the fat pad to the same extent and supported formation of alveoli (Fig. 3 *a* and *b*). The fat pads were filled in four of the five *ErbB2*$^{+/+}$ mice and four of the six *ErbB2*$^{-/-}$ mice. Analysis of lactation in transplants after 1 day postpartum is not possible because the transplanted epithelium is not attached to the nipple; apoptosis and remodeling commence rapidly after birth because of the lack of suckling. However, hematoxylin/eosin-stained sections of the glands at 1 day postpartum show similar distended alveoli with milk in the lumens and lipid droplets in the cells, suggesting that both the differentiation and secretory pathways are normal in the +/+ and −/− glands (Fig. 3 *c* and *d*). In addition, the proportion of epithelium relative to stroma is similar in both the +/+ and −/− glands (Fig. 3 *c* and *d*). Both the reconstituted +/+ and −/− glands remodeled normally after pregnancy (Fig. 3 *e* and *f*).

TEBs are sites for proliferation and penetration of the advancing duct into the fat pad at puberty, and they normally regress once the nascent ducts have traversed the mammary fat pad (25). A typical TEB is a bulbous structure at the end of the duct consisting of an outer monolayer of cap cells at the advancing edge that gives rise distally to the myoepithelium surrounding the duct, and an inner compartment of preluminal and luminal body cells that line the duct (Fig. 4 *a* and *c*) (25, 26). In contrast, the *ErbB2*$^{-/-}$ TEBs, although similar in number to the *ErbB2*$^{+/+}$ TEBs, seem to have a normal cap cell/myoepithelial cell layer, but the body cell layer often seems loosely packed, with large spaces, and severely diminished cell number (Figs. 4 *b*, *d*, and *f* and 5 *b*, *d*, *f* and *h*). This

Table 1. Analysis of whole mounts, seven weeks after transplantation

	Scored in same recipients*		Scored in all recipients†	
	+/+ $n = 3$	−/− $n = 3$	+/+ $n = 4$	−/− $n = 6$
Length of total outgrowth in glands‡	8.41 ± 1.5	5.04 ± 1.4	8.41 ± 1.2	5.41 ± 1.1
Branch points per unit area§	29.7 ± 17.2	48.7 ± 9.3	26.0 ± 13.3	48.8 ± 8.4

*Results in animals in which both +/+ and −/− transplants were successful, permitting direct comparison.
†Results for all successful transplants, regardless of status of contralateral gland.
‡The average end-to-end length of total ductal outgrowth at 7 weeks posttransplantation measured in arbitrary units, with standard deviation ($P = 0.0449$ for same recipient and $P = 0.0036$ for all recipients).
§The average number of branch points within a defined area, with standard deviation ($P = 0.1678$ for same recipient and $P = 0.0174$ for all recipients).

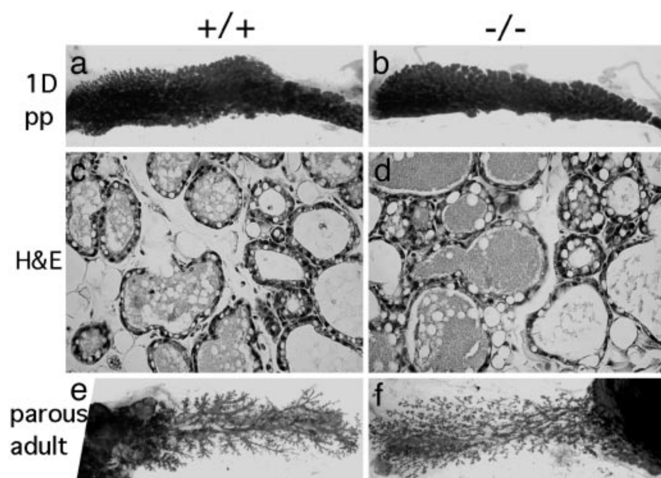

Fig. 3. Whole mount analysis of lobuloalveolar development and remodeling of transplanted glands. Mammary buds from day 13.5 embryos (+/+ or −/−) were transplanted into the cleared no. 4 inguinal fat pads of a 3-week-old recipient mouse. The mouse was mated 4 weeks posttransplantation and delivered a litter 7 weeks posttransplantation. The glands were harvested 1 day postpartum (1D pp). The half-glands (produced by cutting lengthwise) are from the same recipient mouse. The *ErbB2*$^{-/-}$ ductal tree (*b*) has filled the fat pad to the same extent as the +/+ transplanted gland (*a*), although there are differences in alveolar morphology; however, there is no difference in the +/+ transplanted gland (*c*) and the *ErbB2*$^{-/-}$ gland (*d*) at the histological level. The *ErbB2*$^{+/+}$ gland (*e*) and the *ErbB2*$^{-/-}$ gland (*f*) are from separate parous nonpregnant females. H & E, hematoxylin/eosin staining.

aberrant TEB phenotype was evident in most or all TEBs in hematoxylin/eosin-stained sections of every *ErbB2*$^{-/-}$ transplanted mammary gland and in none of the *ErbB2*$^{+/+}$ or *ErbB2*$^{+/-}$ transplanted mammary glands. The poor outgrowth of *ErbB2*$^{-/-}$ transplanted glands at 4 weeks made it difficult to identify TEBs (Fig. 2*b*). Direct comparisons of TEBs from *ErbB2*$^{-/-}$ transplants with those of *ErbB2*$^{+/+}$ or *ErbB2*$^{+/-}$ transplants were difficult at later time points, e.g., 7 weeks, because the wild-type TEBs regress at times when *ErbB2*$^{-/-}$ ducts have only minimally penetrated the fat pad (e.g., Fig. 2 *c*, regressed, vs. *d*). Therefore, detailed comparisons of TEBs were made between the 4-week +/+ outgrowths and the 7-week −/− outgrowths.

Proliferating cells are normally enriched in the cap cell layer and the outer layers of body cells (BrdUrd incorporation, Fig. 4*e*) (27). BrdUrd-positive cells are present in the *ErbB2*$^{-/-}$ TEB cap cell and body cell layers (Fig. 4*f*). The percentage of BrdUrd-positive cells did not differ significantly between the *ErbB2*$^{+/+}$ and *ErbB2*$^{-/-}$ outgrowths, with 19.3 ± 9.4% BrdUrd-positive cells in *ErbB2*$^{+/+}$ TEBs and 17.2 ± 9.1% in *ErbB2*$^{-/-}$ TEBs. However, the *ErbB2*$^{-/-}$ TEBs, with fewer cells overall, had fewer BrdUrd-positive cells. Analysis of apoptosis rates was inconclusive for *ErbB2*$^{-/-}$ TEBs, owing to the small cell numbers.

SMA is expressed by cap cells and myoepithelial cells, but not by body cells (28). *ErbB2*$^{+/+}$ TEBs display normal SMA immunostaining (Fig. 5*a*), with the single outer layer of the TEBs staining. The small number of SMA-positive cells located interiorly are thought to be cap cells that have migrated in and are destined for proliferation and/or differentiation into luminal cells (26). In contrast, the *ErbB2*$^{-/-}$ TEBs had many SMA-positive cells within the body cell compartment (Fig. 5*b*). P-cadherin and E-cadherin are adhesion molecules that are differentially expressed in the TEB cell compartments. P-cadherin is expressed in the cap cells and myoepithelial cells, whereas E-cadherin is expressed only by the body cells and is

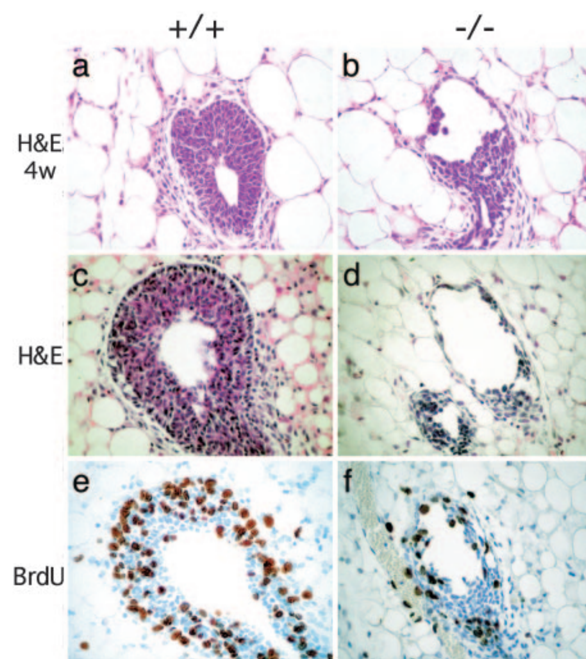

Fig. 4. Morphology and proliferation of TEBs in transplanted glands. (*a* and *c*) TEBs in *ErbB2*$^{+/+}$ and *ErbB2*$^{+/-}$ transplants at 4 weeks posttransplantation have a typical single cap cell/myoepithelial cell outer layer and multilayered body cell compartment. (*a* and *b*) A direct comparison of TEBs from the *ErbB2*$^{+/+}$ and *ErbB*$^{-/-}$ transplants from the same recipient mouse at 4 weeks posttransplantation shows a disorganization of the body cells and a large space between the cap cell and body cell layers. (*d*) The TEBs in *ErbB2*$^{-/-}$ transplants at 7 weeks posttransplantation also show a decrease in the number of body cells and disorganization of the body cells. (*e* and *f*) BrdUrd incorporation in the *ErbB2*$^{+/+}$ TEBs at 4 weeks occurs in both cap and body cells (*e*), but there are fewer BrdUrd-positive cells in the *ErbB2*$^{-/-}$ TEBs at 7 weeks (*f*), concomitant with a smaller cell number ($P = 0.7246$). H & E, hematoxylin/eosin staining.

required for integrity of the body cell compartment (29). In the *ErbB2*$^{+/+}$ TEBs, the cap cells and myoepithelial cells express P-cadherin (Fig. 5*c*, note nearly complete exclusion of inner cell layers), resulting in a similar staining pattern to *ErbB2*$^{+/+}$ TEBs stained for SMA (Fig. 5*a*). Conversely, only the body cells expressed E-cadherin uniformly (Fig. 5*e*, note exclusion of outer cell layer). The *ErbB2*$^{-/-}$ TEBs had many P-cadherin-positive cells in the body cell compartment (Fig. 5*d*) and were heterogeneous for E-cadherin immunoreactivity in the internal layers (Fig. 5*f*). Together, these results suggest an increased body cell infiltration by cap-like progenitor cells in the *ErbB2*$^{-/-}$ TEBs, or altered differentiation in the body cell compartment.

Compartmentalization of the TEB by E-cadherin and P-cadherin status is stabilized through adhesion mediated by binding of netrin-1, produced by prelumenal cells, to the receptor neogenin on the cap cells, which promotes cap cell/prelumenal cell interactions. Loss of netrin-1 or neogenin results in migration of SMA-positive, P-cadherin-positive, E-cadherin-negative cap-like cells into the prelumenal compartment, similar to the phenotype of *ErbB2*$^{-/-}$ TEBs (30). In the *ErbB2*$^{+/+}$ TEBs, the cap cells and myoepithelial cells express neogenin (Fig. 5*g*), resulting in a similar staining pattern to *ErbB2*$^{+/+}$ TEBs stained for SMA and P-cadherin (Fig. 5 *a* and *c*). The *ErbB2*$^{-/-}$ TEBs had neogenin-positive cells in the cap cell and body cell compartment (Fig. 5*h*), in a similar staining pattern to *ErbB2*$^{-/-}$ TEBs stained for SMA and P-cadherin (Fig. 5 *b* and *d*). Neither the cap cell nor body cell layers stained positively for neogenin in tissue from

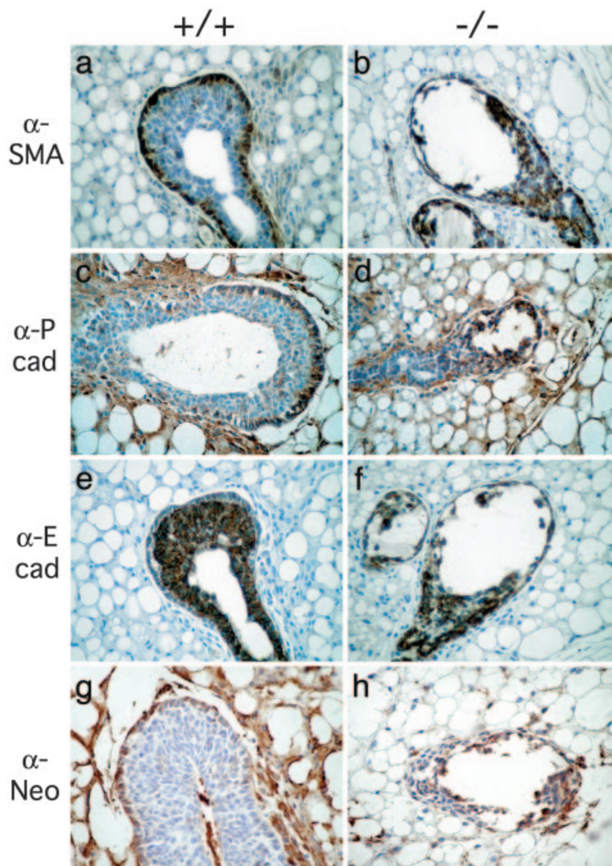

Fig. 5. Immunohistochemical analysis of TEBs. (*a* and *b*) Immunostaining with anti-SMA of glands transplanted with $ErbB2^{+/+}$ donor tissue analyzed at 4 weeks posttransplantation (*a*) and $ErbB2^{-/-}$ donor tissue analyzed at 7 weeks posttransplantation (*b*). (*c–h*) Immunostaining with anti-P-cadherin of glands transplanted with $ErbB2^{+/+}$ donor tissue analyzed at 4 weeks posttransplantation (c) and $ErbB2^{-/-}$ donor tissue analyzed at 7 weeks posttransplantation (*d*); immunostaining with anti-E-cadherin of glands transplanted with $ErbB2^{+/+}$ donor tissue analyzed at 4 weeks posttransplantation (*e*) and $ErbB2^{-/-}$ donor tissue analyzed at 7 weeks posttransplantation (*f*); and immunostaining with anti-neogenin of glands transplanted with $ErbB2^{+/+}$ donor tissue analyzed at 4 weeks posttransplantation (*g*) and $ErbB2^{-/-}$ donor tissue analyzed at 7 weeks posttransplantation (*h*).

$neogenin^{-/-}$ animals (kindly provided by P. Strickland and L. Hinck, University of California, Santa Cruz) (data not shown). However, the loss of ErbB2 did not impede production of neogenin, suggesting that a different signaling system is impaired in *ErbB2*-null transplants. Similarly, immunostaining patterns with anti-netrin were comparable in mammary glands reconstituted with wild-type and $ErbB2^{-/-}$ epithelium (data not shown). Hence, the dysregulation of compartmentalization in TEBs reconstituted from $ErbB2^{-/-}$ tissue does not seem to operate through the netrin/neogenin axis.

Discussion

The lack of ErbB2 in the virgin mammary gland resulted in delayed ductal growth during puberty and adolescence. This phenotype was associated with structural defects of the TEBs. Because in these experiments the recipient fat pad should supply stromal functions, ErbB2 is apparently required in the epithelium. The postnatal contribution of stromal ErbB2 was not addressed in this study. Serial transplants of $ErbB2^{-/-}$ glands harvested 7 weeks posttransplantation were successful, suggesting that null stroma from the original transplant does not contribute significantly to the ductal defect.

A similar ductal penetration defect was evident when floxed ErbB2 was selectively deleted by using a mouse mammary tumor virus (MMTV) transgene (31). However, a TEB defect was not observed, perhaps owing to lack of MMTV-Cre expression in cap cells, or other experimental differences.

At early stages after transplantation, branch points were denser in $ErbB2^{-/-}$ epithelium. Other work has suggested a positive role for ErbBs in branching (32), and TGF-α and neuregulins promote branching (23, 33). The greater branching early after transplantation did not translate to a greater overall number of TEBs. Loss of the most defective $ErbB2^{-/-}$ TEBs might account for this discrepancy and also help to explain the recovery of normal mammary gland morphogenesis as maturation continued.

Structural defects in the TEBs associated with $ErbB2^{-/-}$ epithelium undoubtedly contribute to the ductal penetration defect. Patency of cap/myoepithelial and body cell compartments is maintained by P-cadherin- and E-cadherin-dependent homophilic interactions (29). This compartmentalization is disrupted in $ErbB2^{-/-}$ epithelium. This defect is not due to the loss of the adhesion molecule neogenin, despite the similar structural defects in *neogenin*-null TEBs (30).

The penetration defect could be caused by disruption of the normal regulation of matrix-metalloproteinases (MMPs). Mammary gland branching morphogenesis requires MMP-2 to facilitate TEB invasion and repress precocious lateral branching in mid-pregnancy, whereas MMP-3 is required for secondary and tertiary lateral branching of ducts (34, 35). EGFR has been shown to control branching morphogenesis of the lung by regulating MT1-MMP/MMP14 and MMP-2, a known regulator of normal lung morphogenesis (36). Likewise, ErbB2 signaling could contribute to mammary branching morphogenesis or TEB invasion through one or several MMPs.

ErbB2 is normally activated through growth factor-dependent heteromerization with other ErbBs (14). EGFR and ErbB2 are highly expressed, Tyr-phosphorylated, and colocalized in major cell compartments during ductal morphogenesis, and all four ErbB receptors are expressed and localized to the epithelium during pregnancy and lactation in the mouse mammary gland (15, 16). Of the several EGF family growth factors expressed during mouse mammary development, amphiregulin (AR) seems to be the foremost regulator at puberty, because it is expressed in the virgin mammary gland and promotes ductal morphogenesis when implanted, and because AR knockout mice have a ductal penetration defect that is stronger than disruption of EGF and TGF-α (37, 38). However, TEBs were apparently normal in triple AR, EGF, and TGF-α knockout mice (38). The finding that *EGFR* knockouts have a limiting mammary function in the stroma, not the epithelium (33), seems to contradict the notion that EGFR/ErbB2 interactions are the most important route for ErbB2 activation at puberty. This difference might be explained by the significant methodological differences between the EGFR study and the present one. However, it is possible that the minimal stromal signal can be supplied by EGFR/EGFR homodimers, and that ErbB2 is dispensable in this context. Alternatively, other ErbB receptors may be involved. Because neuregulin-1, which binds to ErbB3 and ErbB4, provokes a strong ductal outgrowth response when implanted in the mammary gland, it is possible that one of these receptors is the functional partner for ErbB2 in this context (23).

At puberty, systemic estrogen works in concert with growth hormone to promote ductal outgrowth (reviewed in ref. 39). Local mediators include insulin-like growth factor 1, fibroblast growth factors, hepatocyte growth factor, and EGF family growth factors (40–42). Further elucidation of the roles of epithelial ErbB2 in integrity of the TEB, and possibly other processes required for ductal elongation (proliferation, sup-

pression of apoptosis, communication with the stroma for regulation of metalloproteinase production), and the placement of ErbB2 in the growth factor regulatory hierarchy will enhance understanding of mammary development and carcinogenesis. The importance of ErbB2 in promoting invasive penetration of the mammary fat pad is consistent with the aggressive properties of mammary carcinoma with *ERBB2* amplification. Better understanding of invasion-related functions of ERBB2 in mammary development may help to explain the frequent amplification of ERBB2 and lead to therapies that target this process in cancer.

We thank Cathrin Brisken, John Wysolmerski, Jeffrey Rosen, Phyllis Strickland, and Lindsay Hinck for protocols and helpful discussions, with special thanks to John and Cathrin for training on transplant techniques. This work was supported by U.S. Public Health Service Grant R01CA45708 (to D.F.S.) and by United States Army Medical Research and Materiel Command Grant DAMD17-99-1-9459 (to A.J.J.-F.).

1. Slamon, D. J., Clark, G. M., Wong, S. G., Levin, W. J., Ullrich, A. & McGuire, W. L. (1987) *Science* **235,** 177–182.
2. Hynes, N. E. & Stern, D. F. (1994) *Biochim. Biophys. Acta* **1198,** 165–184.
3. Holbro, T. & Hynes, N. E. (2004) *Annu. Rev. Pharmacol. Toxicol.* **44,** 195–217.
4. Cobleigh, M. A., Vogel, C. L., Tripathy, D., Robert, N. J., Scholl, S., Fehrenbacher, L., Wolter, J. M., Paton, V., Shak, S., Lieberman, G. & Slamon, D. J. (1999) *J. Clin. Oncol.* **17,** 2639–2648.
5. Yu, D., Suen, T. C., Yan, D. H., Chang, L. S. & Hung, M. C. (1990) *Proc. Natl. Acad. Sci. USA* **87,** 4499–4503.
6. Eccles, S. A. (2001) *J. Mammary Gland Biol. Neoplasia* **6,** 393–406.
7. Muller, W. J., Sinn, E., Pattengale, P. K., Wallace, R. & Leder, P. (1988) *Cell* **54,** 105–115.
8. Guy, C. T., Webster, M. A., Schaller, M., Parsons, T. J., Cardiff, R. D. & Muller, W. J. (1992) *Proc. Natl. Acad. Sci. USA* **89,** 10578–10582.
9. Yarden, Y. & Sliwkowski, M. X. (2001) *Nat. Rev. Mol. Cell. Biol.* **2,** 127–137.
10. Pinkas-Kramarski, R., Soussan, L., Waterman, H., Levkowitz, G., Alroy, I., Klapper, L., Lavi, S., Seger, R., Ratzkin, B. J., Sela, M. & Yarden, Y. (1996) *EMBO J.* **15,** 2452–2467.
11. Tzahar, E., Waterman, H., Chen, X., Levkowitz, G., Karunagaran, D., Lavi, S., Ratzkin, B. J. & Yarden, Y. (1996) *Mol. Cell. Biol.* **16,** 5276–5287.
12. Graus-Porta, D., Beerli, R. R., Daly, J. M. & Hynes, N. E. (1997) *EMBO J.* **16,** 1647–1655.
13. Klapper, L. N., Glathe, S., Vaisman, N., Hynes, N. E., Andrews, G. C., Sela, M. & Yarden, Y. (1999) *Proc. Natl. Acad. Sci. USA* **96,** 4995–5000.
14. Stern, D. F. (2003) *Exp. Cell Res.* **284,** 89–98.
15. Schroeder, J. A. & Lee, D. C. (1998) *Cell Growth Differ.* **9,** 451–464.
16. Sebastian, J., Richards, R. G., Walker, M. P., Wiesen, J. F., Werb, Z., Derynck, R., Hom, Y. K., Cunha, G. R. & DiAugustine, R. P. (1998) *Cell Growth Differ.* **9,** 777–785.
17. Jones, F. E. & Stern, D. F. (1999) *Oncogene* **18,** 3481–3490.
18. Lee, K. F., Simon, H., Chen, H., Bates, B., Hung, M. C. & Hauser, C. (1995) *Nature* **378,** 394–398.
19. Meyer, D. & Birchmeier, C. (1995) *Nature* **378,** 386–390.
20. Morris, J. K., Lin, W., Hauser, C., Marchuk, Y., Getman, D. & Lee, K. F. (1999) *Neuron* **23,** 273–283.
21. Woldeyesus, M. T., Britsch, S., Riethmacher, D., Xu, L., Sonnenberg-Riethmacher, E., Abou-Rebyeh, F., Harvey, R., Caroni, P. & Birchmeier, C. (1999) *Genes Dev.* **13,** 2538–2548.
22. Deome, K. B., Faulkin, L. J., Jr., Bern, H. A. & Blair, P. B. (1959) *Cancer Res.* **19,** 515–520.
23. Jones, F. E., Jerry, D. J., Guarino, B. C., Andrews, G. C. & Stern, D. F. (1996) *Cell Growth Differ.* **7,** 1031–1038.
24. Li, L., Cleary, S., Mandarano, M. A., Long, W., Birchmeier, C. & Jones, F. E. (2002) *Oncogene* **21,** 4900–4907.
25. Silberstein, G. B. (2001) *Microsc. Res. Tech.* **52,** 155–162.
26. Williams, J. M. & Daniel, C. W. (1983) *Dev. Biol.* **97,** 274–290.
27. Humphreys, R. C., Krajewska, M., Krnacik, S., Jaeger, R., Weiher, H., Krajewski, S., Reed, J. C. & Rosen, J. M. (1996) *Development (Cambridge, U.K.)* **122,** 4013–4022.
28. Deugnier, M. A., Moiseyeva, E. P., Thiery, J. P. & Glukhova, M. (1995) *Dev. Dyn.* **204,** 107–117.
29. Daniel, C. W., Strickland, P. & Friedmann, Y. (1995) *Dev. Biol.* **169,** 511–519.
30. Srinivasan, K., Strickland, P., Valdes, A., Shin, G. C. & Hinck, L. (2003) *Dev. Cell* **4,** 371–382.
31. Andrechek, E. R., White, D. & Muller, W. J. (2004) *Oncogene*, in press.
32. Xie, W., Paterson, A. J., Chin, E., Nabell, L. M. & Kudlow, J. E. (1997) *Mol. Endocrinol.* **11,** 1766–1781.
33. Wiesen, J. F., Young, P., Werb, Z. & Cunha, G. R. (1999) *Development (Cambridge, U.K.)* **126,** 335–344.
34. Wiseman, B. S., Sternlicht, M. D., Lund, L. R., Alexander, C. M., Mott, J., Bissell, M. J., Soloway, P., Itohara, S. & Werb, Z. (2003) *J. Cell Biol.* **162,** 1123–1133.
35. Fata, J. E., Werb, Z. & Bissell, M. J. (2004) *Breast Cancer Res.* **6,** 1–11.
36. Kheradmand, F., Rishi, K. & Werb, Z. (2002) *J. Cell Sci.* **115,** 839–848.
37. Kenney, N. J., Smith, G. H., Rosenberg, K., Cutler, M. L. & Dickson, R. B. (1996) *Cell Growth Differ.* **7,** 1769–1781.
38. Luetteke, N. C., Qiu, T. H., Fenton, S. E., Troyer, K. L., Riedel, R. F., Chang, A. & Lee, D. C. (1999) *Development (Cambridge, U.K.)* **126,** 2739–2750.
39. Grimm, S. L., Seagroves, T. N., Kabotyanski, E. B., Hovey, R. C., Vonderhaar, B. K., Lydon, J. P., Miyoshi, K., Hennighausen, L., Ormandy, C. J., Lee, A., *et al.* (2002) *Mol. Endocrinol.* **16,** 2675–2691.
40. Ruan, W. & Kleinberg, D. L. (1999) *Endocrinology* **140,** 5075–5081.
41. Coleman-Krnacik, S. & Rosen, J. M. (1994) *Mol. Endocrinol.* **8,** 218–229.
42. Vonderhaar, B. K. (1987) *J. Cell Physiol.* **132,** 581–584.